Study of Ion Viscosity by Spontaneous L-H Transitions under Marginal Hot Cathode Biasing in the Tohoku University Heliac

S. Kitajima 1), H. Takahashi 1), Y. Tanaka 1), H. Utoh 1), M. Takenaga 1), M. Yokoyama 2), S. Inagaki 2), Y. Suzuki 2), K. Nishimura 2), H. Ogawa 3), M. Takayama 4), J. Shinde 1), M. Ogawa 1), H. Aoyama 1), K. Iwazaki 1), A. Okamoto 1), K. Shinto 1), M. Sasao 1)

1) Department of Quantum Science and Energy Engineering, Tohoku University, Sendai, Japan
2) National Institute for Fusion Science, Toki, Japan
3) Japan Atomic Energy Agency, Naka, Japan
4) Akita Prefectural University, Honjyo, Akita, Japan

E-mail: sumio.kitajima@qse.tohoku.ac.jp

Abstract. The ion viscosity at the L-H transition was estimated in various magnetic configurations by the spontaneous transition condition under the marginal hot cathode biasing in Tohoku University Heliac (TU-Heliac). The critical viscosity, which is the viscosity at the transition point, experimentally estimated from the ***J*** x ***B*** driving force. The critical viscosities in different magnetic configurations agreed with the neoclassical predictions within a factor 2. Although the transition points were spread over a wide range, poloidal Mach numbers at the transition point concentrated near the viscosity maxima predicted by the theory.

1. Introduction

Neoclassical theories explain that the nonlinearity of the ion viscosity plays the important role in the bifurcation phenomena of the L-H transition [1-4] which observed in large tokamaks and stellarators [5-9]. In TU-Heliac the effects of the ion viscosity maxima on the transition to an improved confinement mode have been experimentally investigated by the externally controlled ***J*** x ***B*** driving force for a poloidal rotation using the hot cathode biasing [10-15]. Here, ***J*** and ***B*** are a biasing electrode current and a magnetic field. The biasing experiments for the H-mode transition have been tried in many machines using a cold electrode [16-21]. The electrode current ***J*** of the cold electrode cannot be controlled externally. On the other hand the hot cathode has the advantage to controllability of the electrode currents.

One of further extended works is to clarify the effect of magnetic Fourier components on the neo-classical viscosity. The minimization of helical ripples allows the reduction of viscosity, which is expected to bring good accessibilities to the improved confinement modes. In TU-Heliac the viscosities at the H-L transition point in various magnetic configurations have been evaluated experimentally by *sweeping* the ***J*** x ***B*** driving force and the experimental results showed that the viscosity maxima qualitatively agreed with neoclassical predictions [22] and the hysteresis feature in a driving force were also observed [23]. In these current-sweep-biasing experiments it was difficult to explore precisely the time response of plasma parameters for the transition, because these parameters were actively changed by the electrode current. In order to find a direct trigger on the spontaneous L-H transition observed in large devices, it is appropriate to research plasma parameters at the transition point. In small tabletop machines it is almost impossible to excite the spontaneous H mode. However in TU-Heliac the spontaneous L-H transitions appeared with delay times under the *marginal* biasing condition, which was lower condition than that required for the transition and was precisely tuned by the biasing voltage and heating power for a hot cathode [24].

In this paper we report the poloidal Mach number and the critical ion viscosity which were estimated from the poloidal ***J*** x ***B*** driving force at the spontaneous transition point under the marginal hot cathode biasing in various magnetic configurations which have different maximum viscosities.

2. Experimental set-up in TU-Heliac

The TU-Heliac is a 4-period heliac (major radius, 0.48 m; average plasma radius, 0.07 m). The heliac configurations were produced by three sets of magnetic field coils: 32 toroidal field coils, a center conductor coil, and one pair of vertical field coils. Three capacitor banks consisting of two-stage pulse forming networks separately supplied coil currents of 10 ms flat top [25]. The target plasma for biasing was He plasma produced by low frequency joule heating (f = 18.8 kHz, P_{out} ~ 35 kW). The joule heating power was supplied to one pair of poloidal coils wound outside the toroidal coils [26]. The vacuum vessel was filled with fueling neutral He gas and sealed from the evacuation system before every discharge.

The electrode biasing experiments were carried out using an emissive hot cathode made of LaB_6, which functions as an electron injection source. The LaB_6 hot cathode (diameter, 10 mm; length, 17 mm) was inserted horizontally into the plasma from the low magnetic field side at a toroidal angle $\phi = 270°$ as shown in Fig. 1. In the A-B poloidal cross-section, the flux surface was bean- or kidney-shaped. The hot cathode was heated by a floating power supply and a negative bias voltage was applied against the vacuum vessel by a voltage-control power supply. The biasing condition was set on the lower condition than that required for the transition and was precisely tuned by the biasing voltage and the heating power for the hot cathode.

The radial profiles of electron temperature, density, plasma potential, and the fluctuation levels were measured with a triple probe at a toroidal angle $\phi = 0°$. The line density along a vertical chord through the magnetic axis was measured with a 6 mm microwave interferometer at $\phi = 90°$. The radial distributions of the fluctuation level in a floating potential and an ion saturation current were measured with a rake probe at $\phi = 90°$. The visible light emission was monitored using 25 cm and 1 m spectrometers at $\phi = 158°$ and 338°. The plasma flow velocity was measured by a Mach probe at $\phi = 158°$. The typical plasma parameters before biasing were as follows. The electron density on the magnetic axis was 6×10^{17} m^{-3} and the electron temperature on the axis was about 20 eV. The average radius of the last closed flux surfaces were about 6 ~ 7 cm. The magnetic field on the axis was 0.3 T.

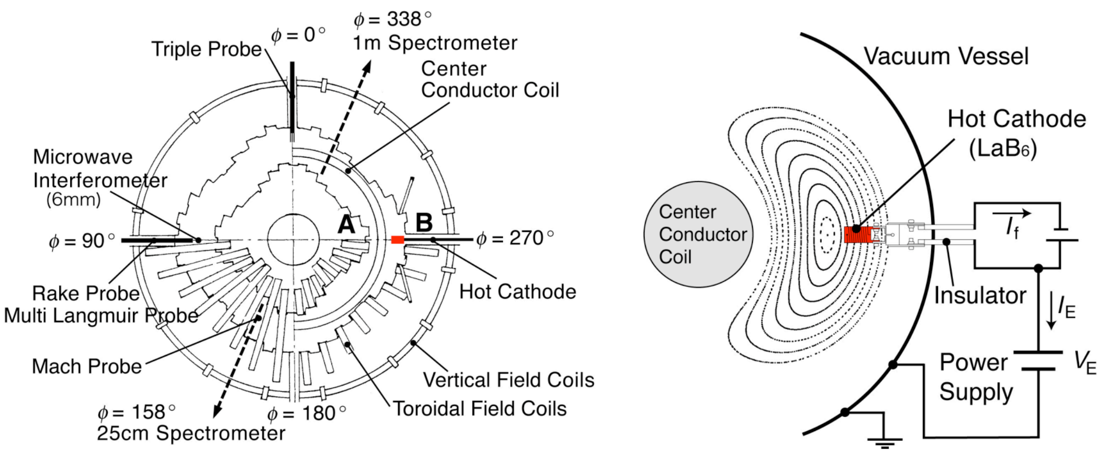

FIG. 1. Experimental set-up in TU-Heliac.

3. Experimental results of *marginal biasing*

Figure 2 shows the time evolutions of plasma parameters under the marginal hot cathode biasing. The bias voltage was fixed at ~200 V with a *constant voltage* power supply. The He plasma produced by low frequency joule heating was negatively biased from the beginning to the end of discharge (Fig. 2a). The electron density, temperature and space potential were measured with the triple probe. With a delay of ~ 5 ms after the start of biasing, the plasma space potential suddenly dropped followed by increases in the plasma density, stored energy, and electrode current (Fig. 2e, c, d, and b). During the biasing, the electron temperature and the plasma space potential decreased slowly until the transition (Fig. 2d, e). Figure 3 shows the time evolutions of electrode current in which the delay times were different even though the biasing conditions were fixed. The delay times of spontaneous transitions were sensitive to the initial phase of a plasma production. The delay time was sufficiently long to saturate the electron density and the electrode current.

We measured the plasma flow around the transition point with a Mach probe. Figure 4 shows the time trace of the Mach probe signal, which is the ratio of ion saturation currents I_{s1}/I_{s2}. During the biasing, the ratio I_{s1}/I_{s2} also increased gradually until the transition and increased suddenly at the transition.

The fluctuation behaviors were explored with the Langmuir probe. Figure 5 shows the normalized power spectrum of fluctuation in the ion saturation current. Here, fluctuation level was normalized with an averaged ion saturation current. We cannot see the significant change in the fluctuation before the spontaneous transition ($t <$ ~ 5 ms). The fluctuation level in the frequency range $f < 50$ kHz was suppressed after the transition ($t >$ ~ 5 ms). On the other hand new modes appeared in the higher frequency range $f > 100$ kHz. However the fluctuation level in these modes was less than 10^{-1} ~ 10^{-2} of the level in the frequency range $f < 50$ kHz before the spontaneous transition.

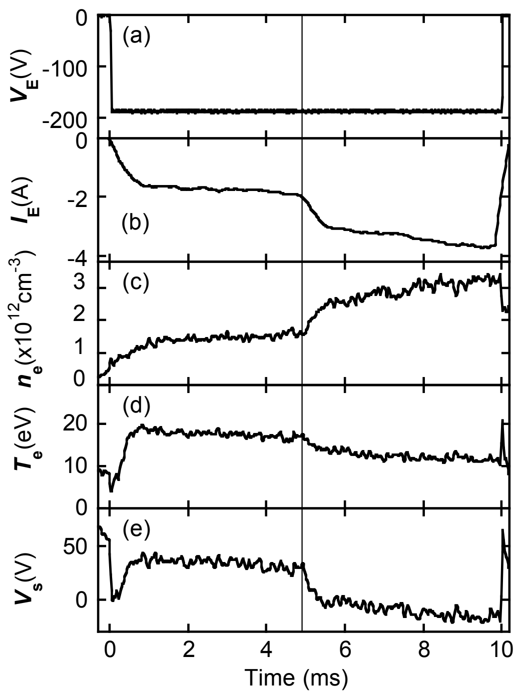

FIG. 2. Typical time evolution of (a) electrode voltage, (b) electrode current, (c) electron density. (d) electron temperature and (e) space potential.

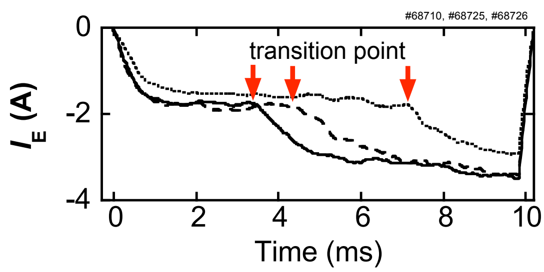

FIG. 3. Typical time evolutions of electrode current in the same biasing condition.

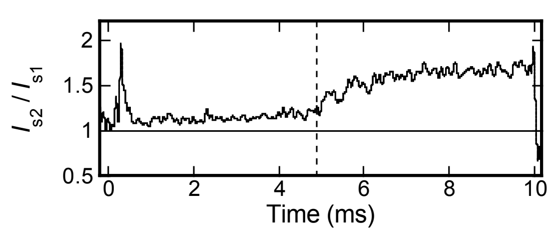

FIG. 4. Time trace of the ratio of ion saturation currents I_{s1}/I_{s2} in the Mach probe signal.

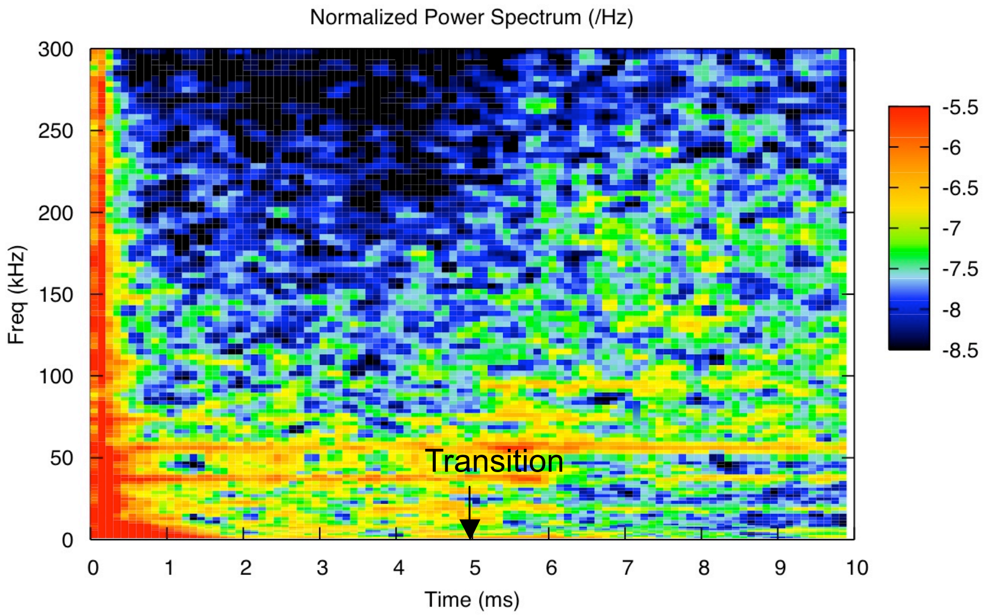

FIG. 5. Normalized power spectrum of fluctuation in the ion saturation current.

These observations indicated that the spontaneous transition was the same transition to the improved confinement mode as the H-mode transition seen in large tokamaks and stellarators.

4. Viscosity estimation in three magnetic configurations

In TU-Heliac the toroidal ripples, helical ripples, and bumpiness are changeable by about 30, 20, and 80%, respectively, by shifting the magnetic axis R_{ax} under a fixed rotational transform profile ($\iota/2\pi = 1.55$ at $\rho = 0$ and 1.75 at $\rho = 1$). Here R_{ax} was the magnetic axis radius measured from the center of the center conductor coil. Main magnetic Fourier components at $\rho = 0.56$, the averaged radius of a last closed magnetic surface and a well depth are shown in Table 1. These flexibilities in magnetic Fourier components lead to slight changes in the relation between ion viscosity and poloidal Mach number M_p. The $\boldsymbol{J} \times \boldsymbol{B}$ driving force for the poloidal rotation balances with the ion viscous damping force and the friction to neutral particles. Therefore the ion viscosity opposing to the poloidal rotation can be estimated experimentally by subtracting the friction term from the driving force.

R_{ax} (cm)	a (cm)	Well depth (%)	ε_{mn} (r = 0.56)		
			(0, 1)	(1, 0)	(1, 1)
7.3	6.3	-0.99	-0.09	-0.049	-0.060
7.5	6.6	-0.11	-0.11	-0.049	-0.056
7.9	6.8	2.3	-0.13	-0.040	-0.051
8.4	6.2	4.1	-0.16	-0.039	-0.050

TABLE 1. Main magnetic Fourier components at ρ = 0.56, the averaged radius of a last closed magnetic surface and a well depth.

We estimated the poloidal Mach number M_p at the spontaneous transition point in 3 configurations (R_{ax} = 7.7, 7.9 and 8.4 cm) and we show the relation between the poloidal Mach number and the delay time of the transition points in Fig. 6. Here, the definition of the poloidal mach number is $M_p \equiv E_r/B_p v_{th}$ and $v_{th} \equiv (2T_i/m_i)^{1/2}$. E_r, B_p, m_i and T_i are the radial electric field, the poloidal magnetic field, the ion mass and temperature. The poloidal Mach number was calculated from the radial electric field which was translated to the averaged value for the mean minor radius from the local electric field measured by the rake probe. In Fig. 7 we show the critical viscosities at $\rho = 0.56$ estimated at the spontaneous transition point in 3 configurations (R_{ax} = 7.7, 7.9 and 8.4 cm). The ion viscosities calculated from Shaing Model [4] are also shown in Fig. 7. Although the transition points shown in Fig. 6 were spread over a wide range, poloidal Mach numbers evaluated at the transition point concentrated around $1< -M_p < 2$ near the viscosity maxima. It seems that when the poloidal Mach number reaches some critical value, the spontaneous transition appears.

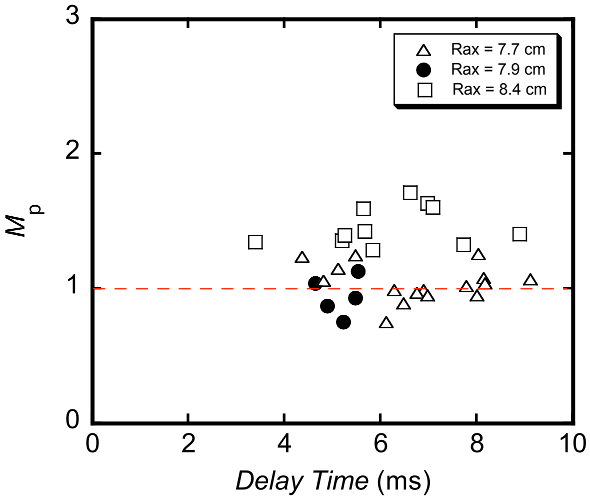

FIG. 6. Relation between the poloidal Mach number and the delay time of the transition points in 3 configurations (R_{ax} = 7.7, 7.9 and 8.4 cm).

We compared the measured critical viscosity with the maximum value in the calculated ion viscosity for 4 configurations (R_{ax} = 7.3, 7.7, 7.9 and 8.4 cm) in Fig. 8. We adopted the charge exchange cross-section in the literature [27] in order to subtract the friction term from the ***J*** x ***B*** driving force. The ion viscosity was comparable to the friction in the poloidal Mach number region where the spontaneous transition appeared, thus the experimentally evaluated viscosity includes large ambiguity affected from the friction estimation. The mean value in 3 configuration cases agreed with the calculated maximum viscosity within a factor of 2 and that of R_{ax} = 8.4 cm was lower than other. These were consistent with the results in the

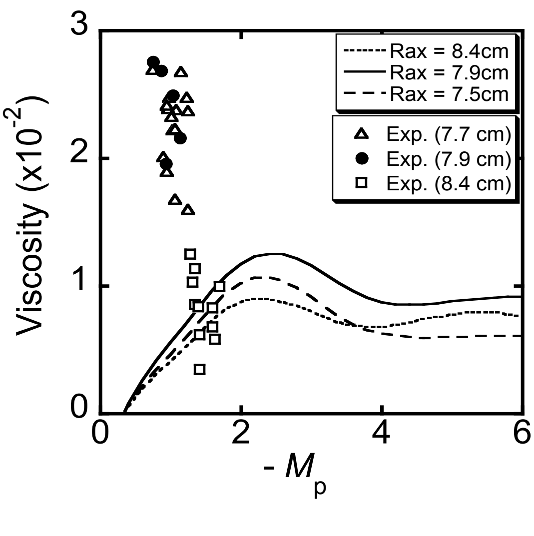

FIG. 7. Critical viscosities evaluated experimentally at spontaneous transition point and ion viscosities calculated from the Shaing model.

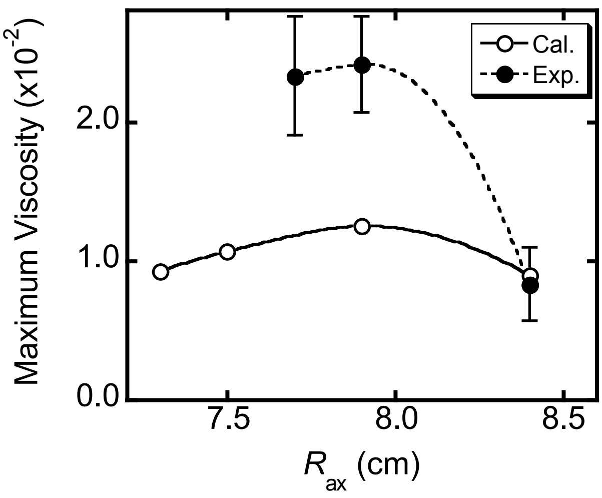

FIG. 8. Dependency of neo-classical ion viscosity on the magnetic axis position and experimentally evaluated viscosities. The vertical error bars indicate the deviation of data points.

externally forced biasing, *i. e.* current-sweep-biasing experiments [28].

5. Summary

Spontaneous transition conditions were explored, and poloidal Mach numbers and the critical ion viscosity in 3 magnetic configurations were estimated under the *marginal* hot cathode biasing. The biasing experiments under the marginal conditions were appropriate to research plasma parameters at the transition point.

(1) Poloidal Mach numbers experimentally evaluated at the transition point concentrated around $1 < -M_p < 2$ near the viscosity maxima, although the transition points were spread over the wide range.

(2) The mean value of critical viscosity in 3 configurations agreed with the calculated maximum viscosity within a factor of 2. The deduced ion viscosities at the spontaneous transition point were consistent with the results in the externally forced biasing, *i.e.* current-sweep-biasing experiments [28].

Acknowledgments

The authors are grateful to Dr K Itoh, Dr K Ida, Dr Y Kamada and Dr Y Miura for helpful discussions. This work was supported by a Grant-in-Aid from the Ministry of Education, Science and Culture of Japan (No 17360439) and in part by the LHD Joint Planning Research programme at the National Institute for Fusion Science.

References

[1] Itoh S.-I., Itoh K. 1988 *Phys. Rev. Lett.* **60** 2276
[2] Shaing K.C., Crume J.E.C. Jr. 1989 *Phys. Rev. Lett.* **63** 2369
[3] Shaing K.C. 1993 *Phys. Fluids* B **5** 3841
[4] Shaing K.C. 1996 *Phys. Rev. Lett.* **76** 4364
[5] Wagner F. *et al* 1982 *Phys. Rev. Lett.* **49** 1408
[6] Burrell K.H. *et al* 1987 *Phys. Rev. Lett.* **59** 1432
[7] Erckmann V. *et al* 1993 *Phys. Rev. Lett.* **70** 2086
[8] Kotschenreuther M. *et al* 1995 *Phys. Plasmas* **2** 2381
[9] Toi K. *et al* 1996 *Plasma Phys. Control. Fusion* **38** 1289
[10] Inagaki S. *et al* 1997 *Japan. J. Appl. Phys.* **36** 3697
[11] Kitajima S. *et al* 2002 *Int. J. Appl. Electromagn. Mech.* **13** 381
[12] Tanaka Y. *et al* 2003 *J. Plasma Fusion Res. Ser.* **6** 371
[13] Kitajima S. *et al* 2006 *Nucl. Fusion* **46**, 200
[14] Tanaka Y. *et al* 2006 *Plasma Phys. Control. Fusion* **48** A285
[15] Kitajima S. *et al* 2006 *Fusion Science and Technology* **50**, 201
[16] Taylor R.J. *et al* 1989 *Phys. Rev. Lett.* **63** 2365
[17] Weynants R.R. *et al* 1990 *Nucl. Fusion* **30** 945
[18] Askinazi L.G. *et al* 1992 *Nucl. Fusion* **32** 271
[19] Wang E.Y. *et al* 1995 *Nucl. Fusion* **35** 467
[20] Dahi H., Talmadge J.N., Shohet J.L. 1998 *Phys. Rev. Lett.* **80** 3976
[21] Van Oost G. *et al* 2003 *Plasma Phys. Control. Fusion* **45** 621
[22] Rozhansky V., Tendler M. 1992 *Phys. Fluids* B **4** 1877
[23] Takahashi H. *et al* 2006 *Plasma Phys. Control. Fusion* **46,** 39
[24] Kitajima S. *et al* 2006 *Plasma Phys. Control. Fusion* **48** A259

[25] Kitajima S. *et al* 1991 *Japan. J. Appl. Phys.* **30** 2606
[26] Kitajima S. *et al* 2001 *J. Plasma Fusion Res. Ser.* **4** 391
[27] F. C. Barnett ed: *Collisions of H, H_2, He and Li Atoms and Ions with Atoms and Molecules*, ORNL-6086, Vol. 1, A-72shed at JPFR SERIES **6** [Proc. ITC13].
[28] Takahashi H. *et al* 2003 *J. Plasma Fusion Res. Ser.* **6**, 366